INTERNATIONAL JOURNAL OF CONSERVATION SCIENCE
ISSN: 2067-533X Volume 14, Issue 3, July-September 2023: 937-954 www.ijcs.ro
DOI: 10.36868/IJCS.2023.03.10

SEM-FEG-EDS, GC-MS, EPR AND VIBRATIONAL SPECTROSCOPY ANALYSIS OF MATERIALS IN BAROQUE-STYLE SCULPTURE "*OUR LADY OF SORROWS*" FROM GAROPABA, SANTA CATARINA, BRAZIL

Thiago G. COSTA[1, 2,*], Adolfo HORN Jr. [2], Lino MEURER[1, 2], Rafaela da Silva BARBOSA[1,2], Fábio A. RICHTER[1], Felipe de A. BEIRÃO[1], Gustavo Amadeu MICKE[2], Samantha GONÇALVES[2], Bruno SZPOGANICZ[2], Mayara R. FORNARI[3], Tassya T. da Silva MATOS[3], Antônio S. MANGRICH[2, 3]

[1] Laboratory of Materials, Atelier for the Conservation-Restoration of Movable Cultural Heritage, Fundação Catarinense de Cultura (Santa Catarina Culture Foundation), 88025-200 Florianópolis, SC, Brazil
[2] Department of Chemistry, Federal University of Santa Catarina (UFSC), 88040-900 Florianópolis, SC, Brazil
[3] Departament of Chemistry, Federal University of Paraná (UFPR), 81531-980, Curitiba, PR, Brazil

Abstract

Materials belonging to the polychromy and gilding of the sculpture 'Our Lady of Sorrows, which belongs to the collection of a church in Garopaba, Santa Catarina, southern Brazil, were analyzed by multiple techniques. The analysis by μ-Raman and FTIR indicated the use of the ultramarine blue pigment, confirmed by EDS, with calcium carbonate observed in the base of preparation. The results show the use of gold leaf based on a gold and silver alloy, and the use of Armenian bole with clay and traces of manganese, as the base for fixing the gold leaf was characterized. GC-MS analysis suggested the use of plant oil in the painting process. Finally, the EPR analysis showed the presence of Fe^{3+}, Mn^{2+} and organic radicals from the degradation of the binder, suggesting the formation of complexes with the degradation products, this being one of the first reports in this type of painting.

Keywords*:* Polychrome sculpture; Gilding; Cultural heritage; Spectroscopy; Chromatography.

Introduction

The study of the materials used in pieces of cultural heritage plays a fundamental role in gaining a better understanding of the historical object and aiding decisions regarding its conservation and restoration development. The information obtained through this type of investigation may indicate the presence of past interventions, advanced degradation processes, or even verify the originality of the work [1-2] The application of chemical analysis to cultural heritage is a valuable tool, improving our understanding and interpretation of works of art [1].

Cultural assets belonging to churches in Brazil have a high historical value and represent the rich religious manifestation in the country. Faith in Our Lady of Sorrows (*Nossa Senhora das Dores* in Portuguese) is related to the set of Marian devotions, which are widespread in the scope of the Catholic Church. Folk and iconographic studies have revealed the existence of one hundred and twelve different Marian invocations in Brazil [3]. Devotion and festivities to Our Lady of Sorrows have a long history and were brought by the Portuguese during the

* Corresponding author: thiago_floripa@hotmail.com

colonization of the country [4]. Therefore, there is a need to monitor artistic objects related to the image of *Nossa Senhora das Dores*, due to its high cultural value.

The sculpture of Our Lady of Sorrows, the object of this study, can be seen in Figure 1. It's part of the collection of a church dedicated to São Joaquim in the city of Garopaba, located in Santa Catarina State (southern Brazil). The church originated from the chapel of a whale fishing rig that was active between the years 1793 and 1824 and became the parish church of the city in 1830 [5]. The temple was recognized by the state government as part of the cultural heritage of Santa Catarina State in 1998, and the image of the Church of São Joaquim in Garopaba was acquired in the year of 1876 [5].

Fig. 1. Sculpture of Our Lady of Sorrows, belonging to the Church of São Joaquim in Garopaba, Santa Catarina State, Brazil. Production technique: wood with gilding and polychrome. Dimensions: 992 x 421 x 285 mm

This sculpture has the typology of a retable image, devotional in nature, in a format that is characterized by an emphasis on its dramatic expression, designed to be seen from a distance and in the frontal position [5]. On top of that, the piece can be classified as erudite, following a canon or design related to a certain style, determined by the specific artistic and cultural environment of a time and place [5]. An analysis of the attitude and clothing represented in the image, characterized by the predominance of serenity and restraint, reveals that they are consistent with, according to researchers, the production of religious statues in the 19th century [5].

The aim of the study described herein was to analyze samples of the polychromy of the sculpture of Our Lady of Sorrows, aiming to identify the pigments and other materials present in the sculpture. For pigment analysis, Raman spectroscopy and Fourier transform infrared spectroscopy (FTIR) have become standard analysis techniques due to their sensitivity and applicability to complex matrices, as well they are often used in a complementary way [1, 6, 7].

Equally important, the elemental composition of materials was obtained through scanning electron microscopy with energy dispersive X-ray spectroscopy (SEM-EDS), in order to corroborate the results of the Raman and FTIR spectroscopy, providing a detailed view of the

sample surface [8]. These three techniques are widely used together for the characterization of cultural heritage objects [9-11]. Furthermore, the GC-MS technique was also employed in the study, as it is commonly used for the identification of organic materials, such as binders and drying oils [12-14]. Finally, electronic paramagnetic resonance (EPR) spectroscopy was used to verify the paramagnetic species and the groups that bind to these species.

Experimental part

Materials

All collections were carried out in places with the presence of residues of each material, on the support underneath the sculpture. During the restoration process of the work, the detachment of micro-samples was observed, which were also collected to perform the analysis described herein. Afterward, samples of the colors blue, white, gold, brown and pink were collected, this reflecting all the materials present in the polychromy of the sculpture. Images of the samples were taken with an Olympus SZ51 stereo microscope, as shown in figure 2.

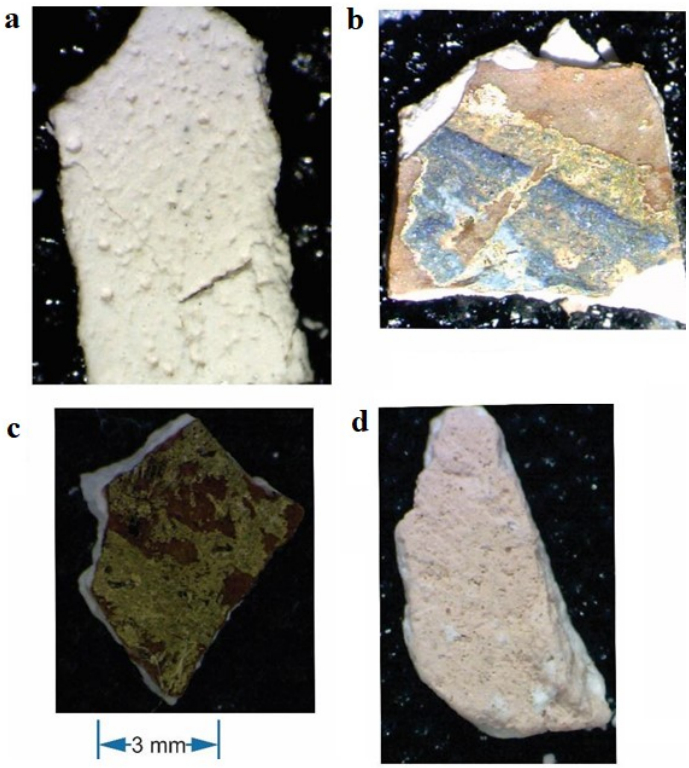

Fig. 2. Microscopic images of fragments of gilding, polychromy and preparation base that were characterized by instrumental analysis: (A) white sample; (B) sample containing gilding, blue polychromy and Armenian bole; (C) gilding sample; (D) pink sample collected from part of the Armenian bole

Figure 3 shows the layers of paint observed in the sculpture. It is observed that the manufacturing of the layers can be divided into two different types of construction: the first is the gilding with polychrome, where the artist used two layers of preparation, plus the polychrome. However, in the base of the sculpture, the artist used only one layer. For more in-depth associations, the materials used in each layer were characterized in this work as well.

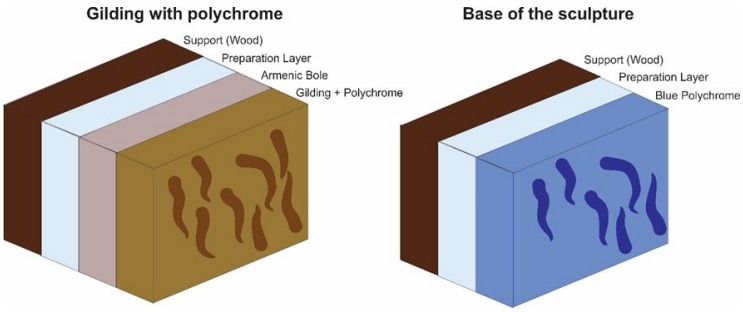

Fig. 3. Layers of the paintings found in the sculpture

Methods

Micro-Fourier transform infrared (FTIR) spectroscopy - μ-FTIR

The samples were analyzed directly on a Shimadzu spectrometer (model IRPrestige-21) coupled with an infrared microscope (AIM-8800), and the detector was cooled with liquid nitrogen. The parameters applied in the analysis were the following: accumulation time of 60 s; objective lens of 15x; wavenumber range at 4000-650cm^{-1} and spectral resolution of 4cm^{-1}.

μ-Raman confocal spectroscopy

The μ-Raman spectra were collected with a Raman confocal WITec alpha 300R microscope using a green laser of 532nm (non-polarized wavelength). The main objective of employing this technique was to assist in the identification and elucidation of the molecular structure of inorganic components used in the sculpture painting.

FEG-SEM with EDS

The field emission gun - scanning electron microscopy (FEG-SEM) with energy dispersive X-ray spectroscopy (EDS) - analysis was performed on a JEOL SEM microscope (model JSM-6701F) with magnification ranging from 140 to 500 times. X-ray diffraction spectra were collected with excitation of 15KeV. This analysis allows the identification of the elements present, their morphology and their distribution in the sample.

EPR spectroscopy

Electron paramagnetic resonance (EPR) analysis was performed with a Bruker EMX spectrometer operating at ~9.5GHz, with 10 Gauss modulation amplitude, 100 kHz modulation frequency, and 5000G (500mT) field scan, at ambient temperature (~300°K). The spectra and g-factor values were obtained using Win-EPR software. The analysis was used to identify paramagnetic metal centers present in the painting materials.

Gas chromatography-mass spectrometry – GC-MS

Chromatography analysis was performed to determine fatty acids using an Agilent chromatograph model 7829, equipped with an automatic injector (model 7683) with electronic pressure control and an Agilent mass detector (model 5975). The programmed temperatures for the detector were: 280ºC for the transfer line, 230ºC for the ion source, 280ºC for the interface and 170ºC for the quadrupole. The programmed mass variation was between 50-900, with a scan time of 20ms. The collision electrons were ionized with 75eV. The operating conditions of the chromatograph were: injection temperature of 250ºC, initial column temperature at 120ºC for 5min, followed by ramping at 10ºC/min up to the final temperature of 300ºC (10 min) with a flow of 1.0mL·min^{-1}, pressure of 9.4 si and linear speed of 41.2m·s^{-1}, using 1 mL of sample injected in splitless mode. A fused silica HP-5 capillary column with dimensions of 30.0m x 0.25mm was used and the film thickness was 0.25mm.

The samples went through a derivatization process as described in the literature with some adaptations: 100mL of the sample was added to a screw cap tube and 2.0mL of a 0.5mol·L^{-1} of NaOH/methanol solution was added. The solution was kept in a boiling water bath for 5min with 2mL of saturated NaCl solution. At the end of this procedure, 2.5mL of

hexane was added, and the solution was stirred for 30s. After decanting, an aliquot of the organic phase was collected for analysis, as described by *T.G. Costa et al*. [15].

Results and discussion

μ-Raman confocal

The composition of the inorganic pigments used in the polychromy was determined from the Raman scattering characteristic of each molecular structure. The Raman spectra for the characterized pigments can be seen in Figure 4. The analysis for the blue layer showed a spectrum with bands at 271, 543 and 1095cm^{-1}, attributed to the ultramarine blue pigment ($Na_{6-10}Al_6Si_6O_{24}S_{2-4}$) [1]. The absence of bands related to calcite can indicate that the pigment used for the painting is of synthetic than rather natural origin, which is consistent with the time that the sculpture was produced, as confirmed by FTIR [16].

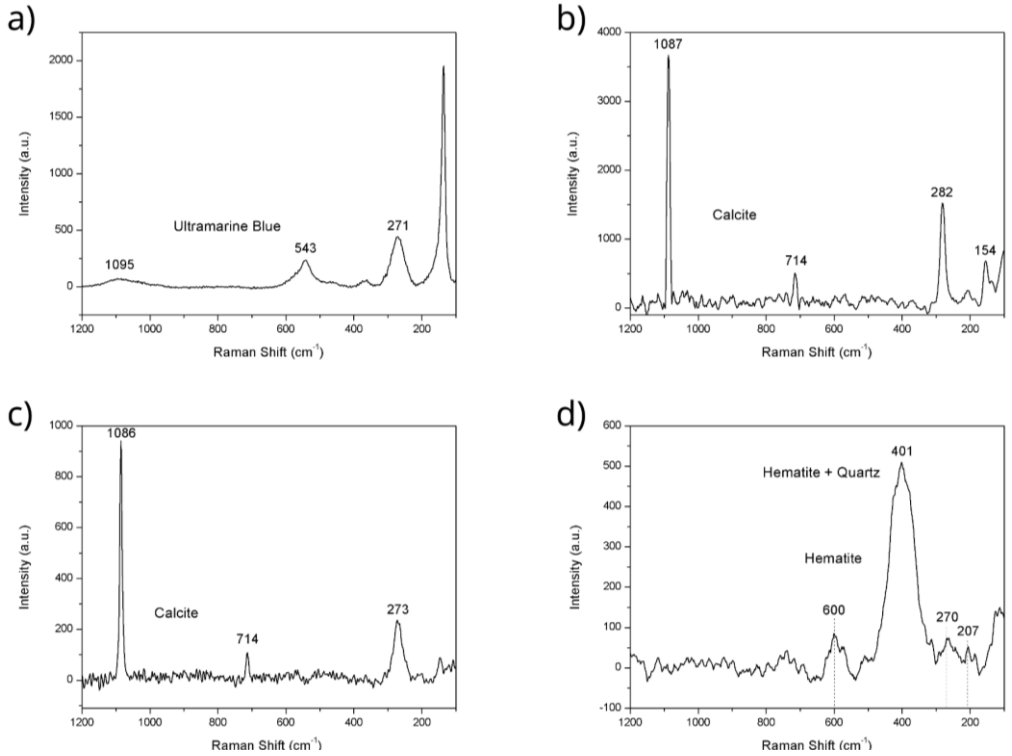

Fig. 4. Raman spectra for the inorganic pigments characterized in the polychrome layers of the sculpture, where (a) = blue; (b) = white, (c) = gilding and (d) = brown

The white layer of preparation of the sculpture had four bands in the Raman spectrum: 154, 282, 714 and 1087cm^{-1}, corresponding to calcite. In the gilding layer, it is possible to observe the presence of only the calcite bands, visible at 154, 282, 714 and 1087cm^{-1}, since the metallic gold alloy does not present bands in the spectrum analyzed [1].

The brown layer had one prominent broadband at 401cm^{-1} and another at 600cm^{-1}. The first value results from the overlapping of the characteristic bands of hematite and quartz, as the second represents the characteristic band of hematite. Table 1 summarizes the bands obtained for the samples analyzed and the respective designations.

Table 1. Main bands found in the Raman spectra and their relationship with the characterized pigments

Sample	Raman assignment	Raman shift (cm^{-1})	Characterization	Reference
Blue	Ultramarine	271	Bending vibration (S_3^-)	1,8,16
		543	Symmetrical stretching (S_3^-)	1,16
		1095	Symmetrical stretching (S_3^-)	1,16
White	Calcite	154	External vibration (translational oscillation) CO_3^{2-}	1,8,16-18
		282	External vibration (rotational oscillation) CO_3^{2-}	1,16-19
		714	Bending vibration in the plane: symmetrical deformation of CO_3^{2-}	1,8,16-19
		1087	Symmetrical stretching CO_3^{2-}	1,8,16-19
Gilding	Calcite	147	External vibration (translational oscillation) CO_3^{2-}	1,8,16-18
		273	External vibration (rotational oscillation) CO_3^{2-}	1,8,16-19
		714	Bending vibration in the plane: symmetrical deformation de CO_3^{2-}	1,8,16-19
		1086	symmetrical stretch CO_3^{2-}	1,8,16-19
Brown	Hematite	401	Symmetrical vibration of Fe-O + vibration	1,8,19-20
		600	Symmetrical bending vibration Fe-O	1,8,19-20

Micro-Fourier transform infrared (FTIR) spectroscopy - μ-FTIR

The FTIR analysis, carried out to complement the Raman spectroscopy, confirmed some of the results described in the previous section. The spectra for the layers analyzed can be seen in Figure 5. For the blue sample, bands were observed at 910, 1008, 1031 and 1101cm^{-1}, with the last three overlapping, which corresponds to the stretching of the Si-O bond and Si-O-Al of the blue pigment used in the blue layer.

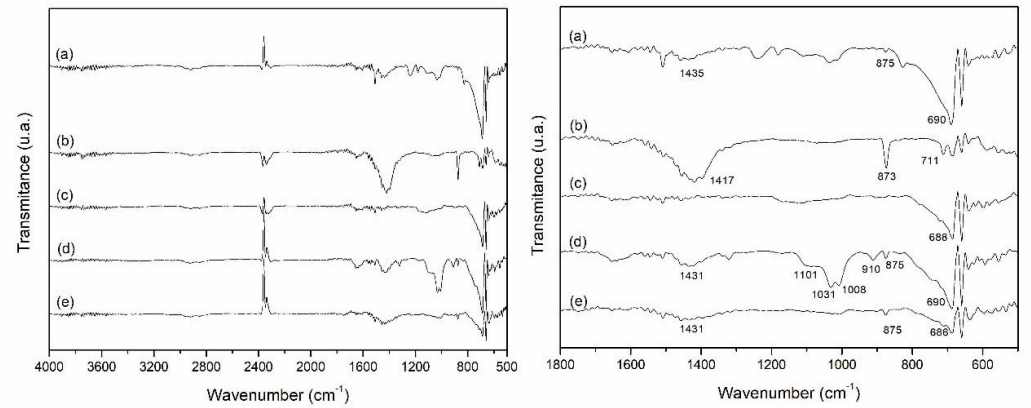

Fig. 5. FTIR spectra for the polychrome layers: (a) white, (b) pink, (c) gold, (d) blue and (e) brown

The presence of characteristic bands of calcite at 690, 875 and 1431cm^{-1}, related to the carbonate stretching, are possible to be observed as well. The presence of carbonate can be attributed to the white lead used to give different tones in painting, knowing that Pb was identified in the EDS spectrum.

The white sample showed bands at 690, 875 and 1435cm^{-1}, which correspond to the asymmetric stretching of calcite carbonate, being the presence of carbonate consistent with the basic components found in paint preparation surfaces. In the golden sample, it is not possible to

observe the presence of gold or silver that can be used for the gilding alloy, since absorption bands in the studied infrared region would not be present.

The brown sample also showed bands associated with calcite at 689 and 875cm^{-1}, along with bands in the region of 650-530cm^{-1}, corresponding to hematite. It should be noted that absorption bands typical of hematite can also appear at wavenumbers smaller than 500cm^{-1}, not obtained in this analysis due to instrumental limitations [11, 21-22]. The pink sample showed bands similar to the white sample at 686, 711, 873 and 1417cm^{-1}, related to the carbonate stretching. Bands associated with hematite were not seen in the spectrum of this sample, which can be explained by the lower fraction of iron oxide present in this layer. Bands between 3000-2850cm^{-1} were also observed in all spectra, which indicates the presence of organic material in the polychrome layers. Table 2 summarizes the bands obtained for the samples analyzed and their respective designations.

Table 2. Attribution of bands observed on spectra obtained by the μ-FTIR

Sample	Wave-number (cm^{-1})	Assignment	Characterization	Reference
Blue	690	Calcite	ν4 asymmetric stretching of CO_3^{2-}	1,8,11,19
	875	Calcite	ν2 asymmetric stretching of CO_3^{2-}	1,8,11,19
	910	Ultramarine	Stretching of Si-O-Si	1,23
	1008	Ultramarine	Stretching of Si-O	1,11-14
	1031	Ultramarine	Stretching of Si-O	1,10-11,13
	1101	Ultramarine	Stretching of Si-O-Al	1,11,13-14
	1431	Ultramarine	ν3 asymmetric stretching of CO_3^{2-}	1,8,11,19,23-25
White	690	Calcite	ν4 asymmetric stretching of CO_3^{2-}	1,8,11,19
	870	Calcite	ν2 asymmetric stretching of CO_3^{2-}	1,8,11,19
	1435	Calcite	ν3 asymmetric stretching of CO_3^{2-}	1,8,11
Gilding	688	Calcite	ν4 asymmetric stretching of CO_3^{2-}	1,19,11
Brown	689	Calcite	ν4 asymmetric stretching of CO_3^{2-}	1,19,11
	650-530	Hematite	Stretching of the Fe-O-Fe bond	11,23
	875	Calcite	ν2 asymmetric stretching of CO_3^{2-}	1,11,19
	1431	Calcite	ν3 asymmetric stretching of CO_3^{2-}	1,11,19
Pink	711	Calcite	ν4 asymmetric stretching of CO_3^{2-}	1,11,19
	873	Calcite	ν2 asymmetric stretching of CO_3^{2-}	1,11,19
	1417	Calcite	ν3 asymmetric stretching of CO_3^{2-}	1,11,19

FEG-SEM with EDS

FEG-SEM with EDS analysis was conducted to verify the elements present in the samples, in addition to relating them to the molecular structure characterized by μ-FTIR and μ-Raman. The samples containing the layers of blue, white and gold were also analyzed to determine the elemental distribution in the interface regions between the three distinct shades. The EDS spectrum shows peaks associated with carbon, calcium, oxygen, aluminum, silicon and gold. The presence of calcium carbonate is confirmed by the identification of carbon, calcium and oxygen in the samples. Moreover, the blue pigment is characterized by the presence of aluminum, silicon and oxygen, while the presence of the gold peak indicates the use of gold leaf in the gilding region. Calcite and ultramarine blue were previously characterized by μ-Raman and μ-FTIR. The peaks in sodium, aluminum, silicon and oxygen are due to the presence of the ultramarine blue pigment, observing that peaks associated with sulfur and lead may be superimposed on the spectrum.

The appearance of traces of chlorine and potassium in the EDS spectrum may be attributed to the presence of marine salts adsorbed in the structure of the painting, due to the proximity of the church to the sea. On the other hand, it is possible that the presence of

potassium in the medium is due to the type of calcium carbonate used, resulting of the potassium uptake by the calcite structure during its precipitation [9, 26].

The spectrum also allows the identification of lead in the sample, which may indicate the use of lead white in the painting. This is coherent with the presence of carbonate already demonstrated by the μ-FTIR analysis, once lead white contains carbonate in its composition. It was also possible to identify a punctual quantity of barium, whose origin has not been fully determined, and more in-depth investigations are required to evaluate the source of this element in the sample. Following the analysis, the presence of magnesium was identified, originating from calcium carbonate, considering that the literature reports magnesium can be found in calcite when it is not in its pure form [27]. The peaks referring to iron indicate the presence of the oxide as a pigment, and this could have migrated to the layers analyzed. A peak associated with gold was also present, which indicates the use of gold leaf in the gilding region.

The FEG micrograph of the sample allows the observation of the morphological difference between the three shades. The micrograph and the EDS spectrum for gilding can be seen in figure 6.

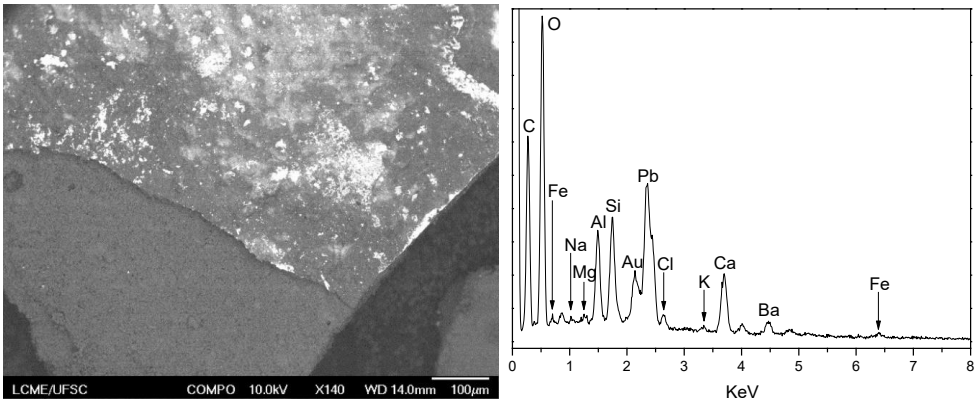

Fig. 6. FEG micrograph and EDS spectrum for the sample containing gilding, blue polychromy and white region

An elemental distribution map was obtained for the sample, showing the location of the elements previously mentioned. Lead is commonly found in white pigments (e.g., lead white or lead carbonate) and, due to its distribution in regions similar to sulfur and sodium, it may have been used in conjunction with the blue pigment in order to obtain lighter shades of blue in the polychrome. This confirms the results obtained from the μ-FTIR spectra, which indicated that another pigment is present in the blue samples, in addition to ultramarine blue. The elemental distribution map is shown in figure 7.

The SEM-FEG micrograph and the EDS spectrum for the white sample can be seen in Figure 8. The peaks obtained show the presence of carbon, oxygen and calcium, confirming the elemental composition of calcium carbonate, in agreement with the results obtained by μ-Raman and FTIR spectroscopy. The elemental distribution map for this sample was not obtained.

The EDS spectrum for the gold-colored sample (Fig. 8) confirm the presence of gold and silver used in the gilding of the work, and not the presence of pigments that resemble gold. Silver is used in the gold alloy to prepare the leaf, improving the mechanical properties of the material. Thereby, this indicates the use of a more noble alloy for gilding, since the presence of other metals, such as copper, results in less noble alloys, with a tendency to present faster degradation of the material [28]. The SEM-FEG micrograph (Fig. 9) of the sample indicates a regular morphology, resembling a metallic surface, as expected for a gold leaf.

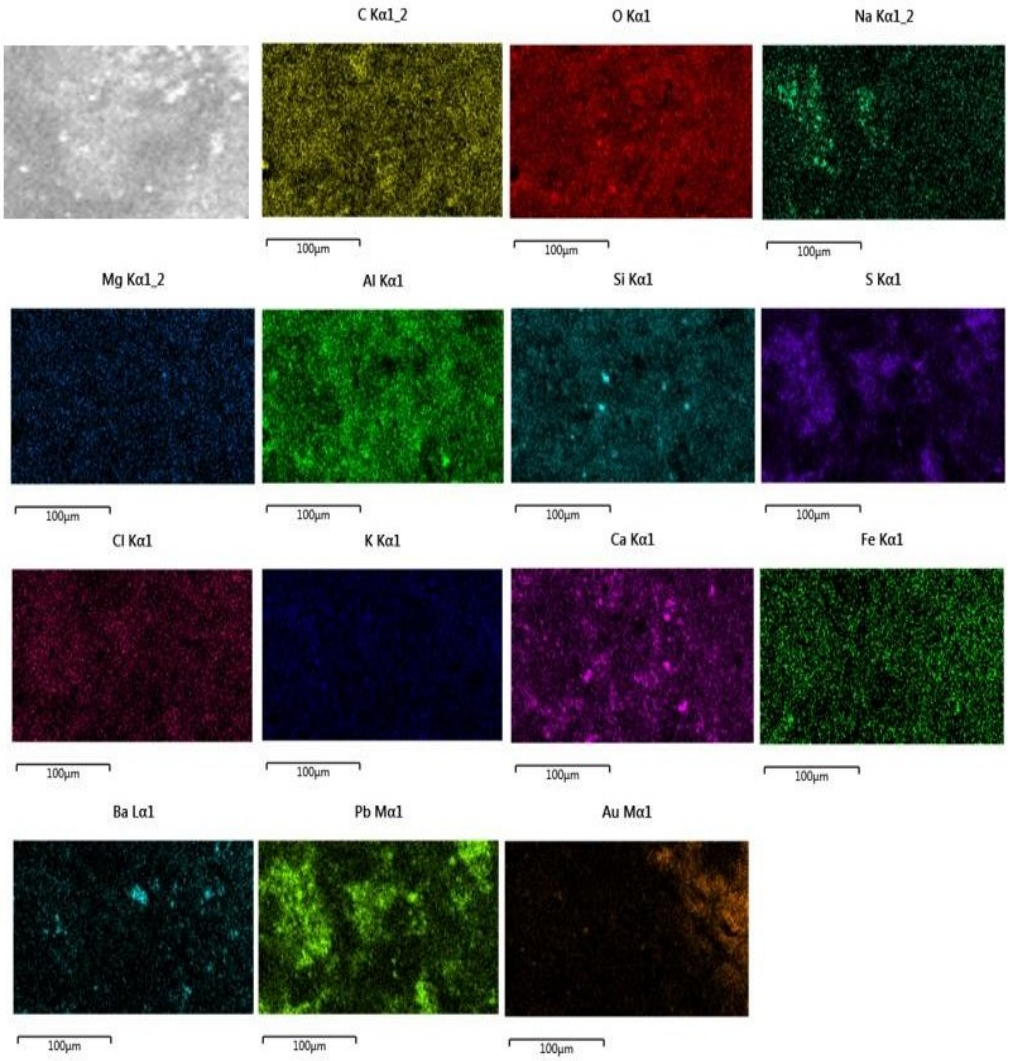

Fig. 7. Elemental distribution map of the blue, white and gold interfaces in the sample

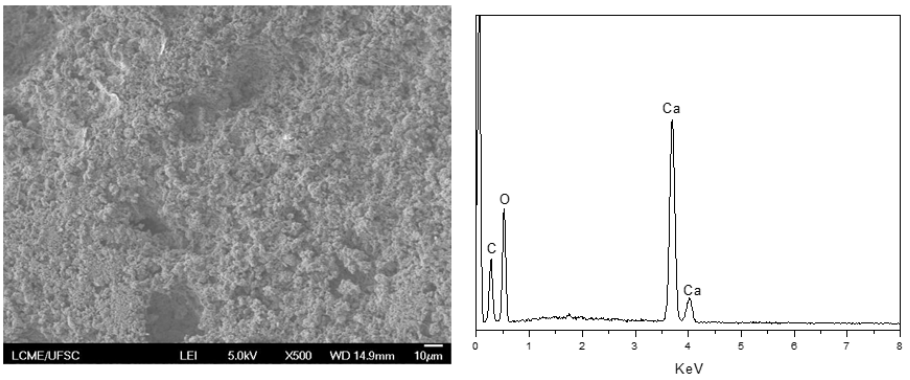

Fig. 8. SEM-FEG micrograph and EDS spectrum for the white sample

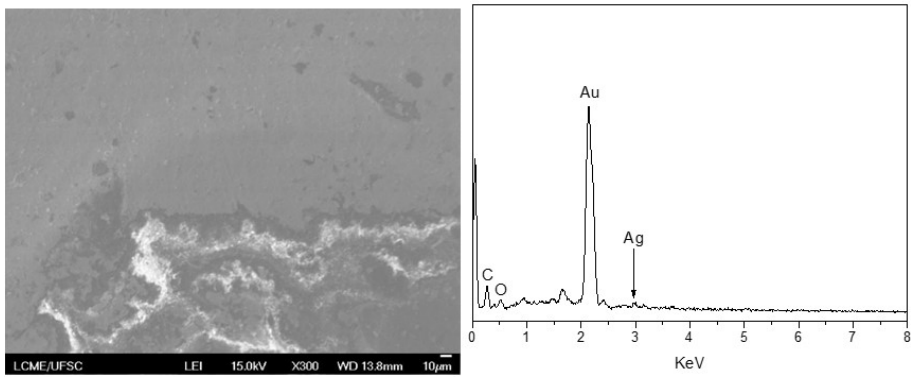

Fig. 9. SEM-FEG micrograph and EDS spectrum for the gilding

From the elemental distribution map of the intersection between the golden and brown layers in Figure 10, it can be seen that the brown sample analyzed contains, in addition to iron, the ultramarine blue pigment. This is due to the concentration of aluminum, silicon and oxygen. The iron comes from the transfer of iron oxide present in the Armenian bole used for the fixation of the gold leaf, possibly during damage to the surface of the gold leaf. Not only, it is also possible to observe a pronounced presence of gold and silver in the smooth part corresponding to the gold leaf, as expected for this type of surface.

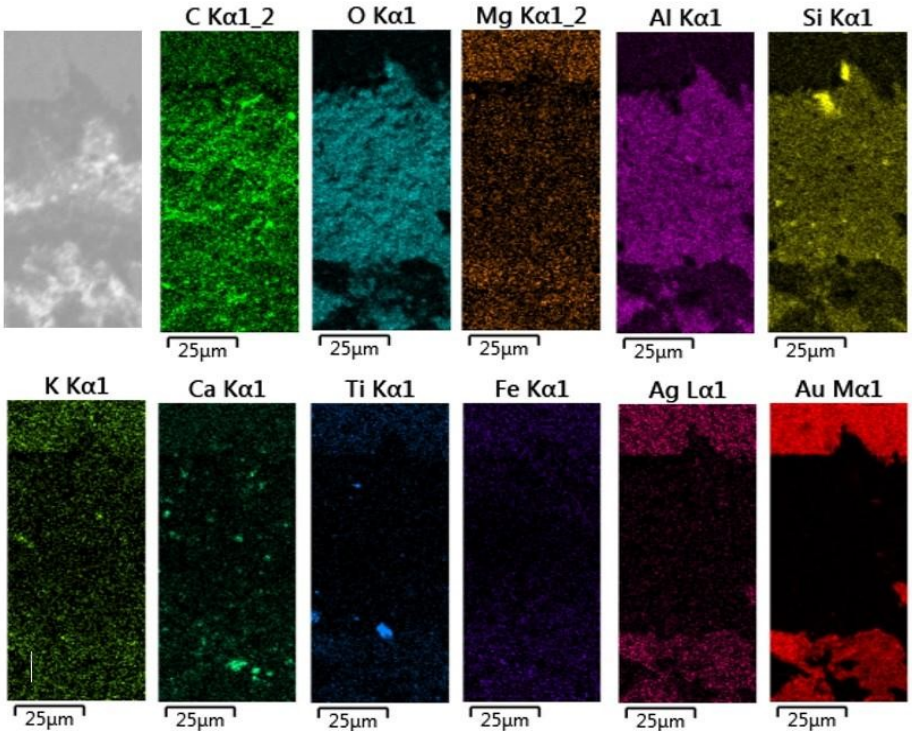

Fig. 10. Elemental distribution map of the intersection of the gilding with the brown layer

In addition, it is possible to observe a diffuse distribution of magnesium, resulting from the transfer of the layer containing calcium carbonate. Likewise, the presence of titanium traces was identified, possibly due to an early restoration process. The presence of magnesium with calcium carbonate can be found in the dolomitic calcite.

The spectrum and micrograph of the pink sample can be seen in Figure 11. Carbon, oxygen and calcium peaks are evident, verifying the presence of calcium carbonate in the sample. The absence of iron in the spectrum obtained for the pink sample, is due to the low quantity or a more diffuse distribution. The SEM-FEG micrograph reveals that the pink layer has a high porosity, a characteristic expected for Armenian bole, since it consists of clay materials together with iron oxides, being used as a fixation layer for the gold leaf.

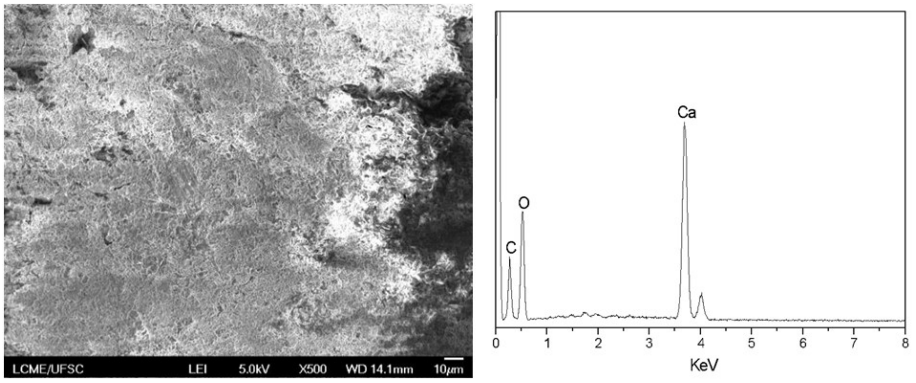

Fig. 11. SEM-FEG micrograph and EDS spectrum for the pink sample

EPR spectroscopy

In pigments, since they contain metals in the form of oxides or complexes, there are usually metal species that have unpaired electrons, a criterion that allows the characterization of this material by electron paramagnetic resonance (EPR) spectroscopy. Through this technique, it is possible to explore the possibility of the presence of metal ions with these requirements, as well as their oxidation states, ligand groups and the possible symmetry of complexes [29]. The spectra for the pink (point fragment of the Armenian bole), gilding and brown samples can be seen in Figure 12.

In the EPR spectrum for the pink sample, a hyperfine split with six lines that are characteristic of Mn^{2+} centers related to the interaction with the nuclear spin (I = 5/2) can be observed. This type of spectrum is characteristic of Mn^{2+} complexes in their solid form, with octahedral geometry and axial symmetry [30-31]. The value of the hyperfine coupling constant identified was A ~ 10mT.

The six lines originated from the nuclear spin of Mn^{2+} in an octahedral site belonging to the Zeeman transitions –5/2 → +5/2, -3/2→ +3/2 e –1/2 → +1/2, respectively [32]. The intermediate lines, which are less intense and appear between these transitions, may be due to prohibited transitions [32], which manifest themselves as a set of doublets between each central transition $|+1/2, m_I\rangle \leftrightarrow |-1/2, m_I\rangle$ [33]. This pink sample was collected from a region of Armenian bole (layer used to fix the gold leaf using earthy pigments with clay materials, a binder and water - a procedure known as water gilding [34]). In addition, the EPR technique is highly sensitive to Mn (II) traces [37] and thus, even in small quantities, its signal can be prominent in the presence of other metals and/or organic free radicals.

In the gilding sample, however, there was a weak signal of organic free radicals with a narrow line, centered at ~ 351mT. In addition, the presence of Fe^{3+} (S = 5/2) is observed through a broad line in the domain concentrated at approximately 321 mT, with a g-factor of ≈ 2.197. According to the literature [37, 38], g-factor values close to 2 indicate that the Fe^{3+} ion is

in the form of oxide or oxyhydroxides. This result represents the possible migration of the iron centers from the brown pigment or from the Armenian bole to the gold layer, with the presence of a radical from the organic binder used for the painting, identified as an oil by GC-MS.

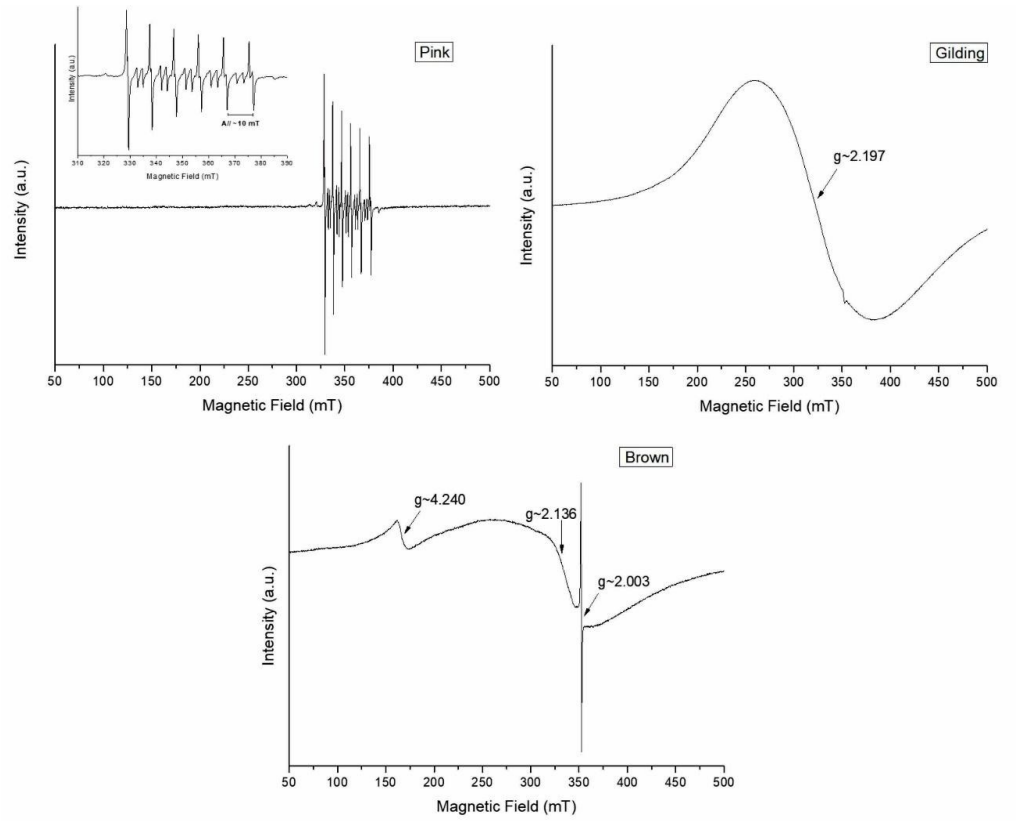

Fig. 12. EPR spectra, magnetic field in the region of 50-500 mT for pink, gilding and brown samples

Finally, the brown paint sample showed signs of organic free radicals, through a narrow and sharp line centered at approximately 353mT, with a g-factor of ≈ 2.003. Following this perspective, the g-factor for these radicals indicates the position of the density of unpaired electrons in view of the chemical bonds between atoms originating from organic matter [29]. A g-factor close to 2.0030 indicates the presence of centered radicals close to carbon atoms and at around 2.0040, the radicals would be centered close to oxygen atoms [39]. There is also the presence of Fe^{3+} ions (S = 5/2) with a wide line in the domain concentrated at 322mT (g ≈ 2.136), and the spectrum shows the presence of Fe^{3+} ions in the domain diluted at 166mT (g ≈ 4.240). The g value close to 4.3 indicates that Fe^{3+} is in rhombic symmetry, while g close to 2 is probably due to the Fe^{3+} ion in the form of oxide or oxyhydroxide [38]. According to the literature [40, 41], these signals are characteristic of Fe^{3+} complexed in octahedral and/or tetrahedral coordination structures with rhombic distortion, whose complexes would be in the presence of organic matter that has functional groups, such as phenols or carboxylic acids. Characterized by the FTIR and μ-Raman analysis, there is the presence of iron oxide as a pigment used for this color. However, the presence of iron complexes that may be associated with the interaction of the iron centers with the residues of iron products was also identified, along with the degradation of the oils used as a binder, obtained by GC-MS [35, 36].

Gas chromatography-mass spectrometry – GC-MS

In order to investigate the presence of oils in the sculpture layers, the samples were analyzed by GC-MS to determine fatty acids, and the results obtained are summarized in Table 3. The analysis indicates the presence of fatty acids, species that could originate from the use of oils as a binder in the paint when applied in the polychrome painting. The hypothesis that the oils used to be of animal origin can be disregarded due to the absence of fatty acids with odd numbers of carbons in the chain and of markers such as cholesterol [42].

Table 3. Composition of fatty acids in the samples and azelaic acid to palmitic acid (A/P) and palmitoleic acid to stearic acid (P/S) ratios

Fatty acids	Gilding, blue and brown	Brown	Gilding	White	Pink
	% of total fatty acids (w/w)				
Lauric acid C12:0	3.56	1.57	2.16	2.49	3.54
Myristic acid C14:0	8.36	2.82	3.54	5.37	5.21
Palmitic acid C16:0	-	48.33	43.08	48.38	57.11
Palmitoleic acid C16:1	-	1.75	2.18	2.93	3.94
Stearic acid C18:0	84.74	41.86	45.36	36.89	27.83
A/P	-	0.0501	0.0506	0.0312	-
P/S	-	1.15	0.950	1.31	2.05

According to the percentages of palmitoleic acid (P) and stearic acid (S), the P/S ratios obtained for the samples are close to the values reported in the literature for linseed oil, even though the highest value obtained suggests a mixture of oils [12-14, 43-44]. However, the P/S value can undergo considerable variations due to the degree of degradation of the material and the presence of pigments and other binders. Knowing that it could also be linked to the chemical cleaning of the work [45].

The presence of fatty acids in the lower layers of the sculpture (white and pink) occurs due to the process of permeation of the polychromy for these layers because of its more porous surface, and significant adsorption of this material. This phenomenon, in addition to the degradation of the paint layer, reflects in the fact that fatty acids, for calculating the P/S ratio, were not identified in the sample containing the fragments of blue, known as the uppermost layer, and thus the values obtained for other samples were used to infer the use of oil in the polychromy.

The presence of azelaic acid (A), a dicarboxylic acid resulting from the oxidation of oils applied in paints, was also identified in the samples, and its ratio with palmitic acid (A/P) may indicate the degree of degradation of the oil used [13]. For all samples in which this substance was identified, the A/P ratios had very low values, which indicates that the oil used is not severely degraded, that is, the constitution of the samples is well preserved.

Because it is a regal image, there is a traditional custom among the faithful to touch it. This touching could lead to the transfer of fatty acids present in tallow and sweat produced by human skin to the surface of the sculpture and, as some lower layers of the work are exposed due to wear and have a porous surface, the adsorption of these acids can easily occur. The presence of fatty acids from this source is confirmed by the detection of palmitoleic acid in the samples, as this circumstance is commonly found in human skin [46, 47]. In such way, the P/S ratios obtained can be influenced by the contamination, by the composition of fatty acids found in these secretions [48-50].

Conclusions

The study described herein provides an overview of the chemical composition of different regions of a polychrome sculpture with gilding called Our Lady of Sorrows. The μ-Raman confocal analysis of the samples allowed the identification of the ultramarine blue

pigment applied to polychromy, suggesting a possible synthetic origin of the pigment, consistent with the date of manufacture of the statue. For the pink and white samples, the presence of carbonate from calcite was observed. Hematite was identified in the brown sample, of earthy origin, due to the presence of quartz.

The FTIR analysis of the samples showed results similar to those obtained by μ-Raman spectroscopy, confirming the presence of ultramarine blue, calcite and hematite in the samples. It was possible to demonstrate that the pink and brown samples are both related to Armenian bole, used as a preparation base for receiving the gold leaf, but with different amounts of iron. The pink sample does not have bands related to hematite, which suggests the use of less hematite in this area of the sample, or even a diffuse distribution of metallic oxides in the preparation of the Armenian bole.

The FTIR results also revealed the presence of organic material in the samples and this is consistent with the data obtained by GC-MS, which indicates the use of an oil in the paint, possibly of a vegetable origin. Due to the state of exposure of the layers analyzed and the tradition of touching sacred images, a factor that promotes the transfer of fatty acids present in the sebum and sweat of human skin, the definitive identification of the composition of the oil used is complex. Above all, the percentage of azelaic acid found in the samples indicates that the layers are in a good state of conservation.

The elements identified by SEM-FEG with EDS for the blue sample (Na, Al, Si and O) correspond to the elemental composition of the ultramarine blue pigment. The presence of Pb was observed, an element that could originate from a pigment added to the color blue to obtain different shades, a hypothesis that has been made consistent with the results of the FTIR spectroscopy, indicating carbonate in the blue sample, since lead carbonates are commonly used as white pigments. In the case of the gold leaf, Au and Ag were identified as components of the metal alloy used, showing that a noble alloy was used for the gilding. The presence of Fe was observed in the brown layer, corroborating the results obtained by μ-Raman and μ-FTIR spectroscopy.

The EPR spectra for the gilding and brown samples showed signs of Fe^{3+}, originating from iron oxides, as confirmed by the μ-FTIR and μ-Raman techniques. The free radicals observed in the EPR analysis may result from the degradation of organic binders present in the paint. In the pink sample, Mn^{2+} was present, this being associated with manganese residues that may be linked to the degradation products of an organic binder present in the paint. Therefore, this was identified as an oil by GC-MS, leading to the possible interaction of iron oxide from pigments with the fatty acids present in the binding. The appearance of this metal was observed only by EPR, demonstrating the importance and sensitivity of this technique.

Finally, the results reported herein provide important information on the sculpture studied, and they could be used to select suitable intervention processes to preserve the sculpture and guarantee its authenticity. In addition, the data contribute to gaining more knowledge regarding the techniques used by artists in the making of sacred works in the 19th century. This highlights the importance of applying chemical analysis in work related to the conservation and restoration of pieces of cultural heritage.

Acknowledgments

The authors would like to thank FAPESC for the scientific initiation scholarship for the student Lino Meuerer, the State of Santa Catarina for the scholarship for student Rafaela da Silva Barbosa and CNPq for the postdoctoral scholarship to researcher Thiago Guimarães Costa – process 101518/2022-6. They are also grateful to the Center for Electronic Microscopy at UFPR and the Central Laboratory of Electronic Microscopy at UFSC. This work was also financed in part by the Coordenação de Aperfeiçoamento de Pessoal de Nível Superior - Brasil (CAPES) - Finance Code 001.

References

[1] B. Stuart, **Analytical Techniques in Materials Conservation**, 1. ed.; John Wiley & Sons Ltd., Sydney, 2007, 424p.
[2] A.M. Committee, *Analysis of historical dyes in heritage objects,* **Analytical Methods**, **13**(4), 2021, pp. 558-562.
[3] J.P. de Souza; R.B. Meira, *A armação baleeira de Garopaba: sua justa dimensão. Florianópolis,* **Esboços**, **25**(40), 2018, pp. 413-434.
[4] J. A. Besen, **1830-1980 São Joaquim de Garopaba (Recordações da Freguesia),** Gráfica e Editora Berthier, Passo Fundo, RS,1980.
[5] R.J.H. Fabrino, **Guia de Identificação de Arte Sacra,** IPHAN, Rio de Janeiro, Brazil, 2012.
[6] R.P. Freitas, I.M. Ribeiro, C. Calza, A.L. Oliveira, V.S. Felix, D.S. Ferreira, A.R. Pimenta, R.V. Pereira, M.O. Pereira, R.T. Lopes, *Analysis of a Brazilian baroque sculpture using Raman spectroscopy and FT-IR,* **Spectrochimica Acta Part A: Molecular and Biomolecular Spectroscopy, 154**, 2016, pp. 67-71. DOI: 10.1016/j.saa.2015.10.013
[7] D. Mancini, A. Percot, L. Bellot-Gurlet, P. Colomban, P. Carnazza, *On-site contactless surface analysis of modern paintings from Galleria Nazionale (Rome) by reflectance FTIR and Raman spectroscopies,* **Talanta, 227**, 2021, Article Number: 122159. DOI: 10.1016/j.talanta.2021.122159
[8] A.M. Hussein, F.S. Madkour, H.M. Afifi, M. Abdel-Ghani, M. Abd Elfatah, *Comprehensive study of an ancient Egyptian foot case cartonnage using Raman, ESEM-EDS, XRD and FTIR,* **Vibrational Spectroscopy, 106**, 2020, Article Number: 102987. DOI: 10.1016/j.vibspec.2019.102987.
[9] S. Bruni, f. Cariati, F. Casadio, L. Toniolo, *Spectrochemical characterization by micro-FTIR spectroscopy of blue pigments in different polychrome works of art,* **Vibrational Spectroscopy, 20**(1), 1999, pp. 15-25. DOI: 10.1016/S0924-2031(98)00096-4.
[10] M. L. Franquelo, A. Duran, L.K. Herrera, M.C.J. de Haro, J.L. Perez-Rodriguez, *Comparison between micro-Raman and micro-FTIR spectroscopy techniques for the characterization of pigments from Southern Spain Cultural Heritage,* **Journal of Molecular Structure, 924**, 2009, pp. 404-402, Special Issue SI. DOI: 10.1016/j.molstruc.2008.11.041
[11] A.K. Marketou, K. Kouzeli, Y. Facorellis, *Colourful earth: Iron-containing pigments from the Hellenistic pigment production site of the ancient agora of Kos (Greece),* **Journal of Archaeological Science: Reports, 26**, 2019, Article Number: 101843. DOI: 10.1016/j.jasrep.2019.05.008
[12] R. Sefcu, V. Pitthard, S. Chlumska, I. Turkova, *A multianalytical study of oil binding media and pigments on Bohemian Panel Paintings from the first half of the 14th century,* **Journal of Cultural Heritage, 23**, 2017, pp. 77-86. DOI: 10.1016/j.culher.2016.10.003.
[13] F. Modugno, F. Di Gianvincenzo, I. Degano, I.D. van der Werf, I. Bonaduce, K.J. van den Berg, *On the influence of relative humidity on the oxidation and hydrolysis of fresh and aged oil paints,* **Scientific Reports**, **9,** 2019, Article Number: 5533. DOI: 10.1038/s41598-019-41893-9
[14] S. Caravá, C.R. Garcia, M.L.V. de Agredos-Pascual, S.M. Mascaros, F.C. Izzo, *Investigation of modern oil paints through a physico-chemical integrated approach. Emblematic cases from Valencia, Spain,* **Spectrochimica Acta Part A: Molecular and Biomolecular Spectroscopy, 240**, 2020, Article Number: 118633. DOI: 10.1016/j.saa.2020.118633.
[15] T.G. Costa, F.A. Richter, E.T. Castro, S. Gonçalves, D.A. Spudeit, G.A. Micke, *Elemental identification of blue paintings traces present in historic cemeteries in the São Martinho*

region, southern Brazil, **Journal of Molecular Structure, 1155**, 2018, pp. 434-442. DOI: 10.1016/j.molstruc.2017.11.027.

[16] I. Osticioli, N.F.C. Mendes, A. Nevin, F.R.C. Gil, M. Becucci, E. Castellucci, *Analysis of natural and artificial ultramarine blue pigments using laser induced breakdown and pulsed Raman spectroscopy, statistical analysis and light microscopy,* **Spectrochimica Acta Part A: Molecular and Biomolecular Spectroscopy, 73**(3), 2009, pp. 525-531. Special Issue SI. DOI: 10.1016/j.saa.2008.11.028.

[17] J. Sun, Z.G. Wu, H.F. Cheng, Z.J. Zhang, R.L. Frost, *A Raman spectroscopic comparison of calcite and dolomite,* **Spectrochimica Acta Part A: Molecular and Biomolecular Spectroscopy,** 117, 2014, pp. 158-162. DOI10.1016/j.saa.2013.08.014.

[18] W.J.B. Dufresne, C.J. Rufledt, J.C.P. Marshall, *Raman spectroscopy of the eight natural carbonate minerals of calcite structure,* **Raman Spectroscopy,** 49(12), 2018, pp. 1999-2007. DOI: 10.1002/jrs.5481.

[19] Y. Yin, W. Zhang, H. Tian, Z. Hu, M. Ruan, H. Xu, L. Liu, X. Yan, D. Chen, *FT-IR and micro-Raman spectroscopic characterization of minerals in high-calcium coal ashe,* **Journal of the Energy Institute, 91**, 2018, pp. 389-396. DOI: 10.1016/j.joei.2017.02.003.

[20] D.L.A. de Faria, F.N. Lopes, *Heated goethite and natural hematite: Can Raman spectroscopy be used to differentiate them?* **Vibrational Spectroscopy, 45**(2), 2007, pp. 117-121. Special Issue SI. DOI: 10.1016/j.vibspec.2007.07.003.

[21] M. Ménager, P.F. Esquivel, P.S. Conejo, *The use of FT-IR spectroscopy and SEM/EDS characterization of slips and pigments to determine the provenances of archaeological ceramics: The case of Guanacaste ceramics (Costa Rica),* **Microchemical Journal, 162**, 2021, Article Number: 105838. DOI: 10.1016/j.microc.2020.105838.

[22] A. Čiuladienė, A. Luckutė, J. Kiuberis, A. Kareiva, *Investigation of the chemical composition of red pigments and binding media,* **Chemija**, **29**(4), 2018, pp. 243-255.

[23] D. Bikiaris, S.X. Daniilia, S. Sotiropoulou, O. Katsimbiri, E. Pavlidou, A.P. Moutsatsou, Y. Chryssoulakis, *Ochre-differentiation through micro-Raman and micro-FTIR spectroscopies: application on wall paintings at Meteora and Mount Athos, Greece,* **Spectrochimica Acta Part A: Molecular and Biomolecular Spectroscopy, 56**(1), 2020, pp. 3-18. DOI: 10.1016/S1386-1425(99)00134-1.

[24] C.E. Silva, L.P. Silva, H.G.M. Edwards, L.F.C. de Oliveira, *Diffuse reflection FTIR spectral database of dyes and pigments,* **Analytical and Bioanalytical Chemistry**, **386**(7-8), 2006, pp. 2183-2191. DOI10.1007/s00216-006-0865-8.

[25] L. Nodari, P. Ricciardi, *Non-invasive identification of paint binders in illuminated manuscripts by ER-FTIR spectroscopy: a systematic study of the influence of different pigments on the binders' characteristic spectral features,* **Heritage Science, 7,** 2019, Article Number: 7. DOI: 10.1186/s40494-019-0249-y.

[26] M. Ishikawa, M. Ichikuni, *Uptake of sodium and potassium by calcite,* **Chemical Geology,** 42(1-4),1984, pp. 137-146. DOI: 10.1016/0009-2541(84)90010-X.

[27] C.H. Moore, W.J. Wade, **Carbonate Reservoirs: Porosity, Evolution and Diagenesis in a Sequence Stratigraphic Framework. Developments in Sedimentology**. 1 ed., Elsevier, Amsterdam, 2001, p. 19-36.

[28] D.A. Scott, *The deterioration of gold alloys and some aspects of their conservation,* **Studies in Conservation, 28**, 1983, pp. 194-203.

[29] T.T.S. Matos, A.S. Mangrich, E.M.C. Cardoso, J. Schultz, M.R. Fornari, A. Wisniewski, I.S.C. Carregosa, *Electron paramagnetic resonance (EPR) spectroscopy as a tool for the characterization of biochar from guava waste,* **Journal of Soils and Sediments, 19**(1), 2018, pp. 286-295. DOI: 10.1007/s11368-018-2048-6.

[30] S.M.M. Romanowski, S.P. Machado, G.R. Friedermann, A.S. Mangrich, M.D. Hermann, H.O. Lima, S. Nakagaki, *Synthesis, Characterization, EPR Spectroelectrochemistry*

Studies and Theoretical Calculations of Manganese (II) Complexes with the Ligands H3bpeten and H3bnbpeten, **Journal of the Brazilian Chemical Society, 21**(5), 2010, pp. 842-850. DOI: 10.1590/S0103-50532010000500011.

[31] A.S. Mangrich, L. Tessaro, A. dos Anjos, F. Wypych, J.A. Soares, *A slow-release K+ fertilizer from residues of the Brazilian oil-shale industry: synthesis of kalsilite-type structures,* **Environmental Geology, 40**(8), 2001, pp. 1030-1036.

[32] C. Castañeda, N.F. Botelho, K. Krambrock, M.S. Dantas, A.C. Pedrosa-Soares, *Centros paramagnéticos em elbaíta rosa natural e irradiada,* **Geonomos**, **14**, 2006, pp. 7-15.

[33] T.A. Stich, S. Lahiri, G. Yeagle, M. Dicus, M. Brynda, A. Gunn, C. Aznar, V.J. DeRose, R.D. Britt, *Multifrequency Pulsed EPR Studies of Biologically Relevant Manganese (II) Complexes,* **Applied Magnetic Resonance, 31**(1-2), 2007, 321-341. DOI: 10.1007/BF03166263.

[34] R. Mayer, **The Artist's Handbook of Materials and Techniques**, 5 ed.; Faber & Faber, 1991.

[35] K. Keune, *Binding medium, pigments and metal soaps characterised and localised in paint cross-sections,* **PhD Thesis**, Swammerdam Institute for Life Sciences (SILS), 2005, available at https://dare.uva.nl/search?identifier=c9e2d8df-e0ad-414e-907d-b615d83cbfe7 accessed in Jul 2021.

[36] J.J. Hermans, K. Keune, A. van Loon, P.D. Iedema, *Toward a Complete Molecular Model for the Formation of Metal Soaps in Oil Paints,* **In Metal Soaps in Art***,* Cultural Heritage Science: Springer, 2019, pp. 47–67. DOI: 10.1007/978-3-319-90617-1_3.

[37] S.L. Reddy, T. Endo, G.S. Reddy, Electronic (Absorption) Spectra of 3d Transition Metal Complexes (Chapter 1) **Advanced Aspects of Spectroscopy**, (Editor: M.A. Farrukh), Tech. Chapt. Publ., 2012. DOI: 10.5772/50128.

[38] S.L. Cogo, A.M. Brinatti, S.C. Saab, M.L. Simoes, L. Martin-Neto, J.A. Rosa, Y.P. Mascarenhas, *Characterization of oil shale residue and rejects from irati formation by electron paramagnetic resonance,* **Brazilian Journal of Physics, 39**(1), 2009, pp. 31-34.

[39] T.T.S. Matos, M.R. Fornari, A.S. Mangrich, J. Schultz, E.M.C.C. Batista, R.O.C. Ribeiro, L.P.C. Romao, C.I. Yamamoto, F.S. Grasel, C. Bayer, J. Dieckow, J.D. Bittencourt, *Low temperature production of biochars from different biomasses: effect of static and rotary lab reactors and application as soil conditioners,* **Journal of Environmental Chemical Engineering, 9(4),** 2021, Article Number: 105472. DOI: 10.1016/j.jece.2021.105472.

[40] L.C. Angelo, A.S. Mangrich, K.M. Mantovani, S.S. dos Santos, *Loading of VO2+ and Cu2+ to partially oxidized charcoal fines rejected from Brazilian metallurgical industry,* **Journal of Soils and Sediments, 14**(2), 2014, pp. 353-359. DOI: 10.1007/s11368-013-0764-5.

[41] S.P. Balena, I. Messerschmidt, J.C. Tomazoni, E. Guimaraes, B.F. Pereira, F.J. Ponzoni, W.E.H. Blum, A.S. Mangrich, *Use of Fe3+ ion probe to study intensively weathered soils utilizing electron paramagnetic resonance and optical spectroscopy,* **Journal of the Brazilian Chemical Society, 22**(9)*,* 2011, 1788-1794. DOI: 10.1590/S0103-50532011000900023

[42] M.P. Colombini; F Modugno; E. Ribechini, *Gas chromatographic and mass spectrometric investigations of organic residues from Roman glass*, (chapter 7), **Organic Mass Spectrometry in Art and Archaeology** (Editors Maria Perla Colombini & Francesca Modugno), John Wiley & Sons, 2009.

[43] E. Manzano, L.R. Rodriguez-Simon, N. Navas, R. Checa-Moreno, M. Romero-Gamez, L.F. Capitan-Vallvey, *Study of the GC–MS determination of the palmitic–stearic acid ratio for the characterisation of drying oil in painting: La Encarnación by Alonso Cano as a case study,* **Talanta, 84**(4), 2011, pp. 1148-1157. DOI: 10.1016/j.talanta.2011.03.012

[44] M.P. Colombini, A. Andreotti, I. Bonaduce, F. Modugno, E. Ribechini, *Analytical strategies for characterizing organic paint media using gas chromatography/mass*

spectrometry, **Accounts of Chemical Research, 43**(6), 2010, pp. 715-727. Special Issue SI. DOI: 10.1021/ar900185f

[45] I. Bonaduce, L. Carlyle, M.P. Colombini, C. Duce, C. Ferrari, E. Ribechini, P. Selleri, M.R. Tine, *New insights into the ageing of linseed oil paint binder: a qualitative and quantitative analytical study,* **PLoS One**, **7**(11), 2012, Article Number: e49333. DOI: 10.1371/journal.pone.0049333.

[46] A. Girod, R. Ramotowski, C. Weyermann, *Composition of fingermark residue: A qualitative and quantitative review,* **Forensic Science International, 223**(1-3), 2012, pp. 10-24. DOI10.1016/j.forsciint.2012.05.018.

[47] E.J. Kim, M.K. Kim, X.J. Jin, J.H. Oh, J.E. Kim, J.H. Chung, *Skin aging and photoaging alter fatty acids composition, including 11, 14, 17-eicosatrienoic acid, in the epidermis of human skin,* **Journal of Korean Medical Science, 25**(6), 2010, pp. 980-983. DOI: 10.3346/jkms.2010.25.6.980.

[48] G.M. Mong, C.E. Petersen, T.R.W. Clauss, **Advanced Fingerprint Analysis Project Fingerprint Constituents,** Pacific Northwest National Lab, Washington, US, 1999.

[49] N. Akaza, H. Akamatsu, S. Numata, M. Matsusue, Y. Mashima, M. Miyawaki, S. Yamada, A. Yagami, S. Nakata, K. Matsunaga, *Fatty acid compositions of triglycerides and free fatty acids in sebum depend on amount of triglycerides, and do not differ in presence or absence of acne vulgaris,* **Journal of Dermatology**, **41**(12), 2014, pp. 1069-1076. DOI: 10.1111/1346-8138.12699.

[50] SS. Shetage, M.J. Traynor, M.B. Brown, M. Raji, D. Graham-Kalio, R.P. Chilcott, *Effect of ethnicity, gender and age on the amount and composition of residual skin surface components derived from sebum, sweat and epidermal lipids,* **Skin Research and Technology**, **20**(1), 2014, pp. 97-107. DOI: 10.1111/srt.12091

Received: September 1, 2022
Accepted: July 10, 2023